X-ray absorption studies of carbon-related materials

W. F. Pong,[a]* C. L. Yueh,[a] Y. D. Chang,[a] M.-H. Tsai,[b] Y. K. Chang,[c] Y. Y. Chen,[c] J. F. Lee,[d] S. L. Wei,[e] C. Y. Wen,[e] L. C. Chen,[e] K. H. Chen,[f] I. N. Lin[g] and H. F. Cheng[h]

[a]Department of Physics, Tamkang University, Tamsui 251, Taiwan, [b]Department of Physics, National Sun Yat-Sen University, Kaohsiung 804, Taiwan, [c]Institute of Physics, Academia Sinica, Taipei 107, Taiwan, [d]Synchrotron Radiation Research Center, Hsin-chu 300, Taiwan, [e]Center for Condensed Matter Science, National Taiwan University, Taipei 106, Taiwan, [f]Institute of Atomic and Molecular Science, Academia Sinica, Taipei 106, Taiwan, [g]Department of Materials Science and Engineering, Materials Science Center, National Tsing-Hua University, Hsin-chu 300, Taiwan, and [h]Department of Physics, National Taiwan Normal University, Taipei 117, Taiwan. E-mail: wfpong@mail.tku.edu.tw

X-ray absorption near-edge structure (XANES) measurements have been performed on nitrogen-doped diamond films with three different dopant concentrations and iron-layer-stabilized carbon nanotube (CNT) structures with various diameters at the C K-absorption edge using the sample drain current mode. The C K-edge XANES spectra of these N-doped diamond films resemble that of the undoped diamond regardless of the dopant concentration, which suggest that the overall bonding configuration of the C atom is unaltered. N dopants are found to reduce the intensities of both the sp^2- and sp^3-bond-derived resonance features in the XANES spectra. On the other hand, the C K-edge XANES spectra of CNTs indicate that the intensities of the π^* and σ^* bands and the interlayer-state features vary with the diameter of the CNT. This phenomenon may be caused by the Fe-layer-catalysed bending of the graphite sheet and the interaction between C and Fe atoms.

Keywords: nitrogen-doped diamonds; carbon nanotubes; XANES.

1. Introduction

Doping of diamond films is of both fundamental and technological interest (Robertson *et al.*, 1999). Several investigations found that boron doping not only improves the quality but also increases the *p*-type conductivity of a diamond film (Won *et al.*, 1996; Liu *et al.*, 1997). Nitrogen was expected to behave as a donor and was found to enhance the electron emission characteristics in diamond films (Okano *et al.*, 1999; Sowers *et al.*, 1999). Meanwhile, the discovery of the tubule form of graphite sheets (Iijima, 1991) has attracted enormous attention over the past decade because of its fundamental and technological interest (Endo *et al.*, 1996; Saito *et al.*, 1998). The formation of carbon nanotubes (CNTs) by chemical vapour deposition using transition metal (TM) catalysts has been investigated extensively (Yudasaka & Kikuchi, 1998; Yudasaka *et al.*, 1997). Theoretical investigations (Kruüger *et al.*, 1998; Duffy & Blackman, 1998; Menon *et al.*, 2000) revealed that the C atoms in the graphite sheet interact strongly with the TM atoms and there is strong hybridization between C *p* and TM *d* orbitals. The charge-transfer effect and the magnetic moment of the TM atoms were found to depend strongly on the metal–graphite interlayer distance and the

adsorption site (Menon *et al.*, 2000). The curvature of the graphite sheet is among one of the factors which were considered to explain the change of the electronic states in CNTs (Mintmire *et al.*, 1992; Blase *et al.*, 1994). Here, we describe X-ray absorption near-edge structure (XANES) measurements at the C K-absorption edge for N-doped diamond films with various N concentrations and attempt to elucidate how the N dopants influence the electronic structures of the diamond films. The C K-edge and the Fe $L_{3,2}$- and K-edge XANES measurements were also performed on CNTs prepared with various Fe layers with different thicknesses.

2. Experimental

The C K-edge and Fe $L_{3,2}$-edge XANES measurements were performed using the high-energy spherical grating monochromator (HSGM) beamline, with an electron-beam energy of 1.5 GeV and a maximum stored current of 200 mA, at the Synchrotron Radiation Research Center (SRRC), Hsinchu, Taiwan. The spectra of the C K edge and Fe $L_{3,2}$ edge were measured using the sample drain current mode at room temperature. For the spectra recorded at the HSGM beamline, the typical resolution was 0.2 eV. The Fe K-edge X-ray absorption measurement was performed in fluorescence mode at the 15B and wiggler beamlines of the SRRC.

Diamond films were grown on silicon substrates by the microwave plasma-enhanced chemical vapour deposition method. Since the N concentration in the diamond film is proportional to the gas-phase urea concentration of the nitrogen source, the variation of the N concentration in the diamond film was obtained by choosing three different urea concentrations, of 3, 4 and 5 sccm, in the preparation process, as described elsewhere (Perng *et al.*, 2000). The CNTs were prepared on *p*-type Si(100) substrates by microwave plasma-enhanced chemical vapour deposition (MPE-CVD). Prior to the MPE-CVD process, thin layers of Fe with various thicknesses were coated on the Si substrate by electron-beam evaporation. Subsequently, CNTs were grown using a microwave power of 1.5 kW at a chamber pressure of 50 torr. Semiconductor-grade CH_4, N_2 and H_2 were used as the source gases and the typical flow rates were 20, 80 and 80 sccm, respectively. The substrate temperature during growth was maintained at approximately 970 K. Using the scanning electron microscope, the randomly oriented multi-wall CNTs prepared with the 30, 150 and 300 Å Fe layers were observed to be around 10 μm in length, and 10 ± 5, 30 ± 15 and 220 ± 100 nm in diameter, respectively, as shown in Fig. 1. The average diameter of the CNT appears to increase with the thickness of the Fe layer coating. Furthermore, as shown in Fig. 2, the transmission electron microscopy (TEM) image clearly shows one Fe cluster which may act as a catalytic growth centre in the nanotube. Details of the preparation procedure for these CNTs will be presented elsewhere.

3. Results and discussion

Fig. 3 displays the C K-edge XANES spectra of N-doped and undoped diamond films. The XANES spectra of the N-doped diamond films prepared with urea concentrations of 3, 4 and 5 sccm, and of the undoped diamond film are denoted as CN_3, CN_4, CN_5 and CN_0, respectively. The spectra were normalized using the incident beam intensity I_0 and by keeping the area under the spectra in the energy range between 335 and 345 eV fixed (not fully shown in Fig. 3). For X-ray energies in the XANES region, the excited photoelectron undergoes a transition from a core level to an unoccupied final state determined by the dipole-transition selection rule. The spectra in Fig. 3 reflect transitions from the C 1*s* core level to unoccupied *p*-like final

states. The spectra of N-doped and undoped diamond films clearly display sharp features closely resembling those reported in earlier works (Morar *et al.*, 1985; Ma *et al.*, 1992). The XANES energy range for diamond can generally be divided into two regions characterized by specific features. One is the spike of the C 1*s* core exciton resonance at approximately 289.2 eV. The other is a relatively broad σ^* feature of the sp^3-bonded C atoms in the energy range between about 290 and 302 eV. The relatively small peak at ~285 eV is usually attributed to the graphite-like π^* state of the sp^2-bonded C atoms, as indicated in Fig. 3. The spectral line shapes in the C *K*-edge XANES spectra of these N-doped and undoped diamond films appear to be nearly identical regardless of the different N concentrations, which indicates that the doping of N atoms in diamond does not significantly alter the overall local environment of the C atom.

The inset of Fig. 3 displays the C *K*-edge electron energy loss spectroscopy (EELS) spectra of two carbon nitride samples containing 25% and less than 1% of nitrogen (Hu *et al.*, 1998*a*,*b*). These two spectra are very different from those of the N-doped diamond films shown in Fig. 3, which indicates that the local bonding configuration of the C atom in N-doped diamond films differs from

that of carbon nitride. In other words, the bonding configuration between the N dopant and the surrounding host C atoms is different from those in carbon nitride.

Fig. 4(*a*) shows the difference intensity curves between the C *K*-edge XANES spectra of the three N-doped samples and that of the undoped sample. Integrations of the intensities over the regions $\Delta A(\pi^*)$ (between 281.6 and 286.1 eV) and $\Delta B(\sigma^*)$ (between 286.1 and 300.7 eV) are plotted in Fig. 4(*b*) as ΔI_{sp^2} and ΔI_{sp^3}, respectively. ΔI_{sp^2} and ΔI_{sp^3} represent N-dopant-induced reduction of the absorption of X-rays by the electron transition from the C 1*s* core state to the unoccupied sp^2 and sp^3 bond states, respectively. Fig. 4(*b*)

Figure 2
Transmission electron microscope image showing a metallic Fe cluster inside the nanotube.
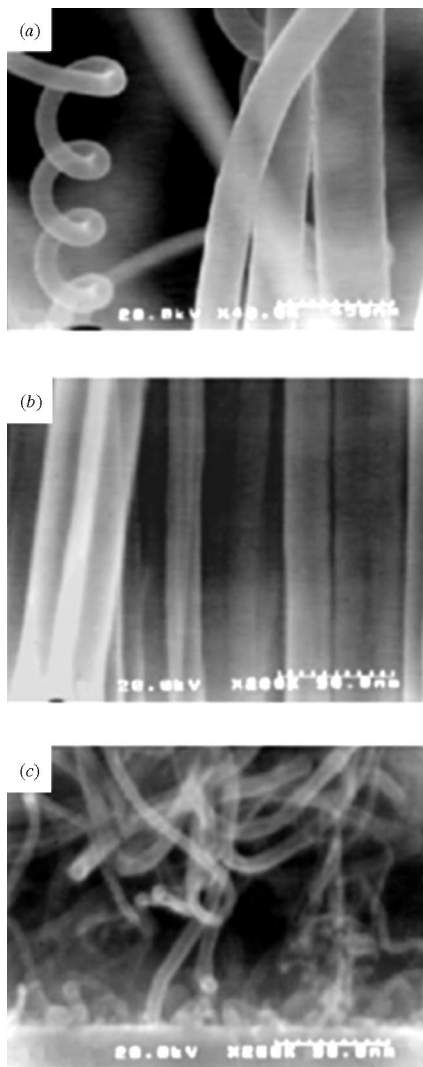
Figure 1
Scanning electron microscope images of the randomly oriented multi-wall carbon nanotubes with diameters of (*a*) 220 ± 100, (*b*) 30 ± 15 and (*c*) 10 ± 5 nm.
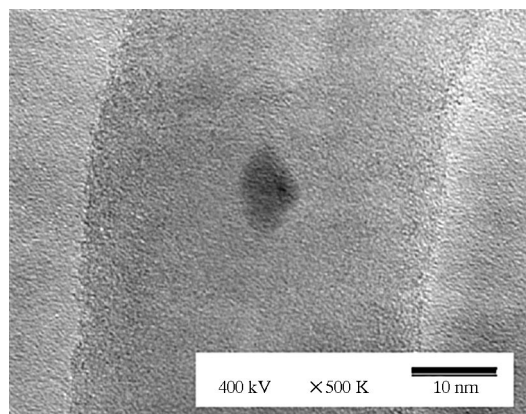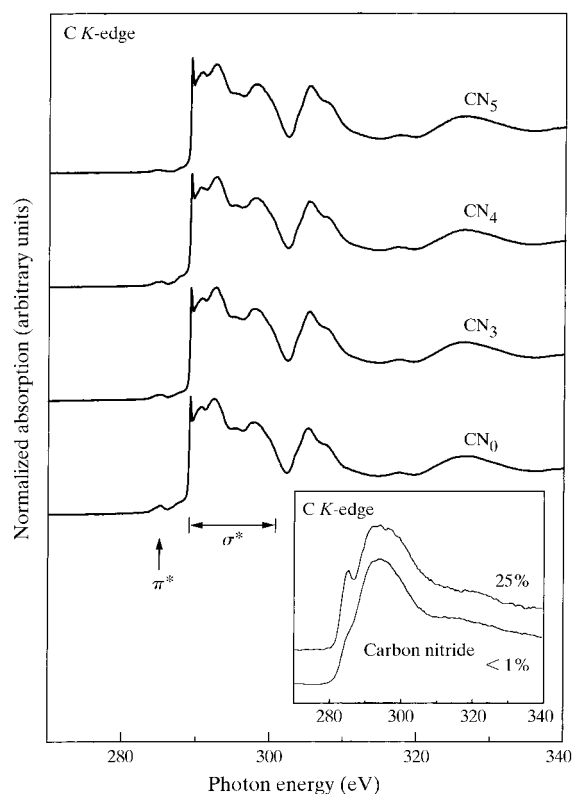
Figure 3
Normalized C *K*-edge absorption spectra of N-doped and undoped diamonds. The inset displays the C *K*-edge EELS spectra of the carbon nitride samples containing less than 1 and 25% of nitrogen (Laikhtman *et al.*, 1999).

shows that ΔI_{sp^2} decreases slightly with the N concentration. In conjunction with the trend of the diminishing π^* feature shown in Fig. 4(a), one can conclude that N dopants suppress the formation of the small quantity of sp^2-bonds in the diamond films, which may exist in the grain boundary regions or on the surface. This is reasonable because N atoms tend to form strong covalent bonds with neighbouring host atoms with directional p orbitals, which may destabilize the planar sp^2 bonding in the diamond films. The same chemical or bonding property of the N atoms may enhance the p-orbital content in the occupied sp^3-bond-derived states in the N-doped diamond films. Consequently, the p-orbital content in the unoccupied sp^3-bond-derived states (or antibonding sp^3 states) will be depleted, so that ΔI_{sp^3} will decrease substantially with the increase of the N concentration, as shown in Fig. 4(b). The present result is in contrast with that obtained for B-doped diamond films, in which the B dopants enhance the number of unoccupied sp^2- and sp^3-bond states (Hsieh *et al.*, 1999).

Fig. 5 displays the C K-edge XANES spectra of the three CNTs prepared with three different Fe layer thicknesses, along with that of the graphite for comparison. The general line shapes in the C K-edge XANES spectra of the three CNTs and the graphite appear to be similar regardless of the different diameters of the CNTs. The two prominent peaks near 285.7 and 292.7 eV are known to be associated with the unoccupied π^* and σ^* bands (Fischer *et al.*, 1991; Batson, 1993), respectively. Between the π^* and σ^* peaks, a weak feature (labelled by a vertical solid line in Fig. 5) near 287.5 eV is also

evident. This feature has not generally been observed in EELS measurements, but has been frequently seen in the X-ray absorption spectra of graphite (Batson, 1993; Pickard, 1997). This feature was attributed to the free-electron-like interlayer states in the graphite (Pickard, 1997). The weak peak that occurs at around 283.5 eV (labelled by a vertical dashed line) was previously attributed to a defect electronic state of the disordered carbon in diamond films (Laikhtman *et al.*, 1999).

The inset of Fig. 5 illustrates the relative intensities of the π^*, σ^* and interlayer-state features for the three CNTs and the graphite. The intensities of the π^* and interlayer-state features are clearly enhanced relative to those of the graphite. Since the intensities of those features are proportional to the density of the unoccupied C $2p$-derived states, the increased intensities of these features can be correlated with the increased unoccupation of the C $2p$ orbitals or a charge transfer from the C $2p$ orbitals to the Fe $3d$ orbitals, as discussed below. This trend suggests that the C $2p$ orbitals in the smaller-diameter CNTs lose more charge to the $3d$ orbitals of the catalyzing Fe atoms than those of the larger-diameter CNTs.

Fig. 6 displays the normalized Fe $L_{3,2}$-edge XANES spectra of the three CNTs with different diameters and the Fe metal. We match the absorption coefficients from the pre-edge region at the L_3 edge to several electronvolts above the L_2 edge and keep the same area in the energy range between 732 and 749 eV. According to dipole-transition selection rules, the dominant transition is from Fe $2p_{3/2}$ and $2p_{1/2}$ to the unoccupied Fe $3d$ states. The area beneath the white line in the Fe
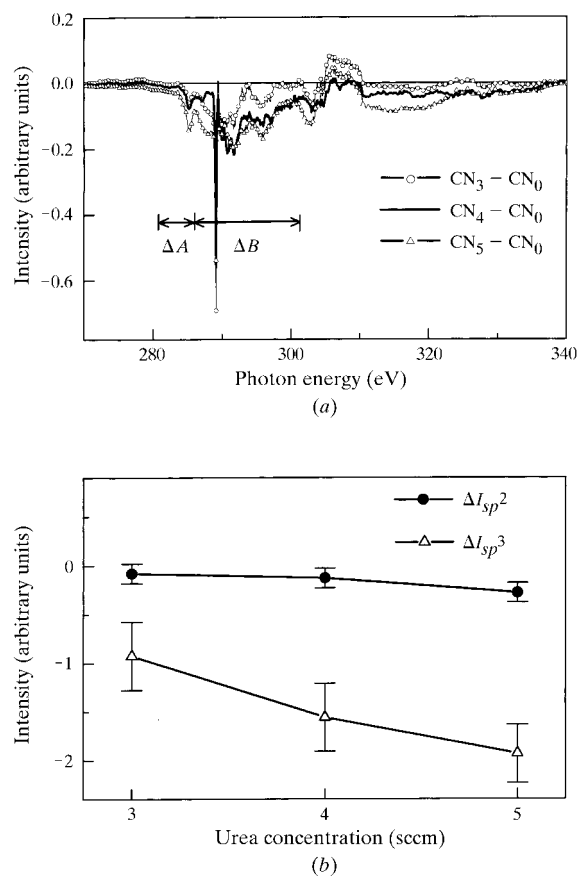

Figure 4
(a) The C K-edge difference intensity curves between N-doped and undoped diamonds. (b) A plot of the integrated difference intensity curves, ΔI_{sp^2} and ΔI_{sp^3}, over regions $\Delta A(\pi^*)$ and $\Delta B(\sigma^*)$, respectively, *versus* N concentration.
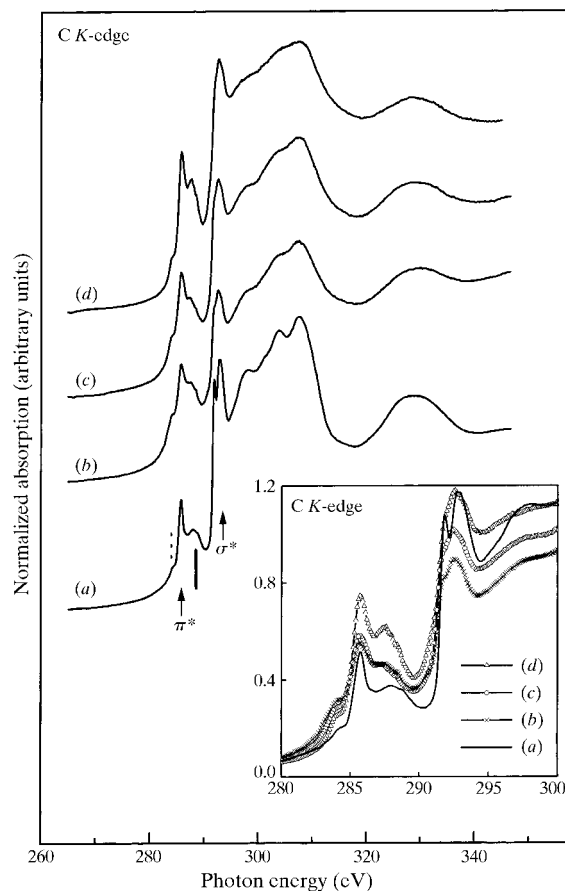
Figure 5
Normalized C K-edge absorption spectra of (a) the graphite and the carbon nanotubes with diameters of (b) 220 ± 100, (c) 30 ± 15 nm and (d) 10 ± 5 nm. The inset displays the enlarged part of the near edge on a magnified scale.

$L_{3,2}$ edge is primarily a convolution of the absolute square of the transition matrix element and the unoccupied densities of states of d character. In Fig. 6, the shapes of the Fe $L_{3,2}$-edge XANES of the CNTs differ significantly from that of the pure Fe metal. The intensities of the CNT white-line features are also significantly smaller than that of the pure Fe (the intensity of the Fe spectrum has been scaled by a factor of 1/2). To understand the dependence of the charge transfer between the C and Fe atoms on the curvature of the graphite sheet in the CNTs, the intensities of the white-line features $I(L_3)$ at the Fe L_3 edge are illustrated in the inset of Fig. 6. $I(L_3)$ is determined by subtracting the background intensity described by an arctangent function, as indicated by the dashed line in Fig. 6. $I(L_3)$ for the CNTs are clearly seen to be significantly lower than that for pure Fe. $I(L_3)$ gradually increases with the diameter of the graphite sheet, suggesting that the number of unoccupied Fe $3d$-derived states increases with the increase of the tube diameter. In other words, the $3d$ orbitals of the Fe atoms in the Fe layer in contact with the smaller-diameter CNT gain more charge from the C $2p$ orbitals than those in contact with the larger-diameter CNT. This result is consistent with that of the C K-edge XANES spectra. The CNT white-line features are clearly accompanied by a lower-intensity peak located just above the Fe L_3 edge. The split peak on the high-energy side is best resolved for the CNT with the largest dia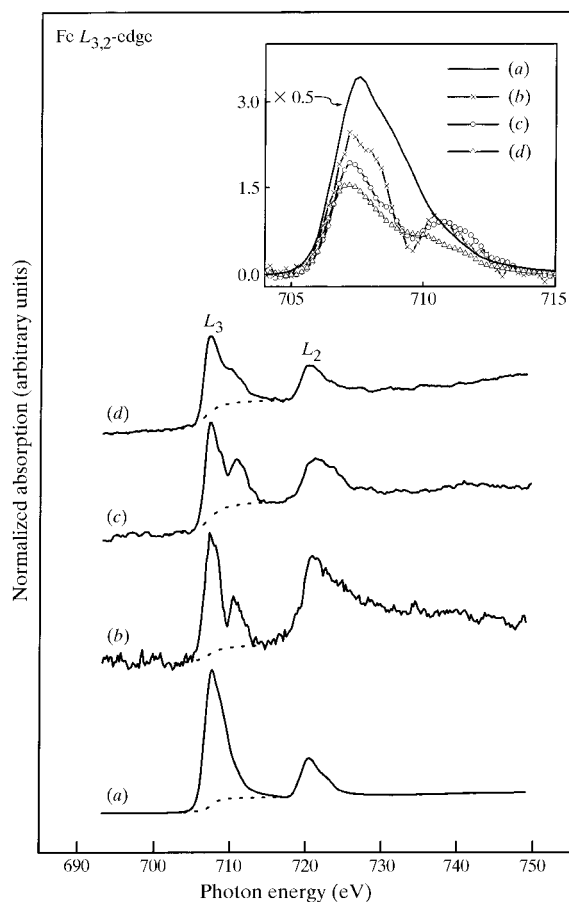meter (220 nm) and it appears to be least resolved for the CNT with the smallest diameter (10 nm). This trend suggests that the hybridization between the C $2p$ and Fe $3d$ states in the graphite sheet increase with the curvature of the CNT, which is consistent with the result of the C K-edge XANES spectra.

The direction of the overall charge transfer between the carbon nanotube and the Fe cluster can be inferred from their work-function difference. The CNT and Fe metal have work functions of 5.3 eV (Hernández et al., 1998) and 4.5–4.8 eV (Lide, 1998), respectively, which indicates that the overall charge transfer should be from the Fe catalyst to the CNT, contrary to the C $2p$ to Fe $3d$ transfer. Thus, there should be other channels of charge transfer that compensate the C $2p$ to Fe $3d$ transfer. One such charge transfer possibly involves rehybridization of the p–d orbitals at the Fe site. To see if this is the case, we carried out Fe K-edge XANES measurements. Fig. 7 shows the normalized fluorescence yield of Fe K-edge XANES spectra of the three Fe-catalyzed CNTs, Fe metal and FeSi. The Fe K-edge XANES spectra reflect transition from the Fe $1s$ core level to the unoccupied Fe p-derived states. The general line shape of the three CNT spectra differs from those in the Fe metal and FeSi, which indicates that the chemical states of the absorbing Fe atom in the CNTs differ significantly from those in pure Fe and FeSi. The absorption intensity for the CNT just above the edge increases as the diameter of the CNT decreases and it is larger than that of pure Fe. This result shows that the CNTs have more unoccupied p-derived states, which suggests that Fe atoms lose p-orbital charge. In addition, the loss of p-orbital

Figure 6
Normalized Fe $L_{3,2}$ near-edge absorption spectra of (a) the Fe metal and the carbon nanotubes with diameters of (b) 220 ± 100, (c) 30 ± 15 and (d) 10 ± 5 nm The dashed line represents the extrapolated background at the Fe L_3 edge. The centre of the continuum step of the arctangent function was selected at the maximum height of the white-line features. The white-line region of the Fe L_3 edge is shown in the inset on a magnified scale. The intensity of the pure Fe spectrum has been reduced by a factor of 1/2.
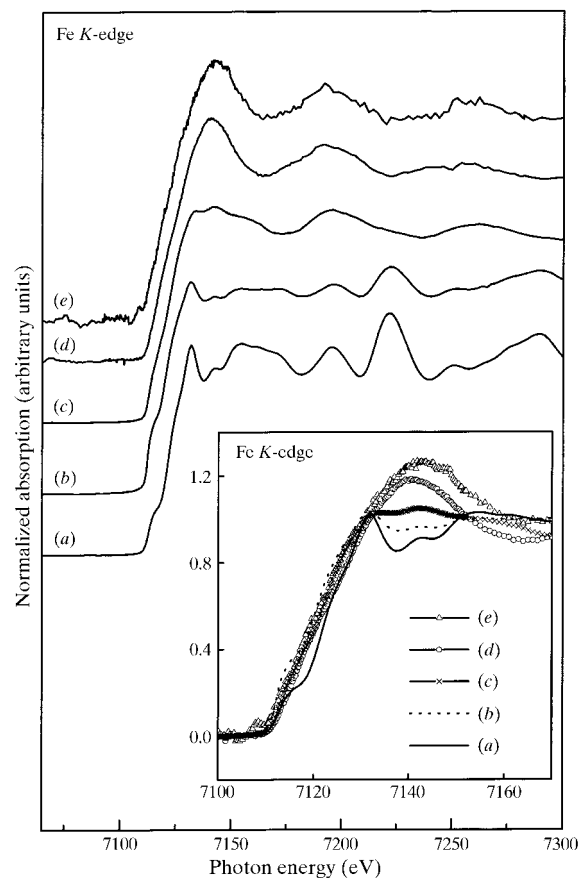

Figure 7
Normalized Fe K-near-edge absorption spectra of the (a) Fe metal, (b) FeSi, and the carbon nanotubes with diameters of (c) 220 ± 100, (d) 30 ± 15 and (e) 10 ± 5 nm. The region of the threshold edge in the inset is on a magnified scale. (The data for Fe metal and FeSi were measured using the total electron yield mode.)

charge increases with the decrease of the nanotube diameter. Thus, the gain in the $3d$-orbital charge may be compensated by the loss in p-orbital charge at the Fe site.

4. Summary

In summary, the comparison between the C K-edge XANES spectra of N-doped diamond films and those of the carbon nitride samples suggests that the local bonding configuration of the host C atoms surrounding the N dopant in the N-doped diamond film is very different from that in the carbon nitride. An analysis of the changes of the C K-edge XANES spectra of N-doped diamond films shows that the N dopants reduce the number of unoccupied sp^3 states. The C K-edge XANES spectra of the CNTs studied indicate that the intensities of the π^* and σ^* bands and the interlayer-state features vary with the diameter of the CNT. This phenomenon can be caused by the bending of the graphite sheet and the interaction between C atoms and the Fe atoms. The white-line features at the Fe L_3 edge suggest a strong hybridization between the C $2p$ and Fe $3d$ orbitals and a certain degree of charge transfer between the C $2p$ and Fe $3d$ orbitals depending on the CNT diameter. Our Fe K-edge measurements reveal a p–d rehybridization effect that reduces p-orbital occupation at the Fe site.

References

Batson, P. E. (1993). *Phys. Rev. B*, **48**, 2608–2610.
Blase, X., Benedict, L. X., Shirley, E. L. & Louie, S. G. (1994). *Phys. Rev. Lett.* **72**, 1878–1881.
Duffy, D. M. & Blackman, J. A. (1998). *Phys. Rev. B*, **58**, 7443–7449.

Endo, M., Iijima, S. & Dresselhaus, M. S. (1996). *Carbon Nanotubes*. Oxford: Pergamon.
Fischer, D. A., Wentzcovitch, R. M., Carr, R. G., Continenza, A. & Freeman, A. J. (1991). *Phys. Rev. B*, **44**, 1427–1429.
Hernández, E., Goze, C., Bernier, P. & Rubio, A. (1998). *Phys. Rev. Lett.* **80**, 4502–4505.
Hsieh, H. H., Chang, Y. K., Pong, W. F., Tsai, M.-H., Chien, F. Z., Tseng, P. K., Lin, I. N. & Cheng, H. F. (1999). *Appl. Phys. Lett.* **75**, 2229–2231.
Hu, J., Yang, P. & Lieber, C. M. (1998*a*). *Appl. Surf. Sci.* **127–129**, 569–593.
Hu, J., Yang, P. & Lieber, C. M. (1998*b*). *Phys. Rev. B*, **57**, R3185–R3188.
Iijima, S. (1991). *Nature (London)*, **354**, 56–58.
Kruüger, P., Rakotomahevitra, A., Parlebas, J. C. & Demangeat, C. (1998). *Phys. Rev. B*, **57**, 5276–5280.
Laikhtman, A., Gouzman, I., Hoffman, A., Comtet, G., Hellner, L. & Dujardin, G. (1999). *J. Appl. Phys.* **86**, 4192–4198.
Lide, D. R. (1998). *CRC Handbook of Chemistry and Physics*, 79th ed. New York: CRC.
Liu, K., Zhang, B., Wan, M., Chu, J. H., Johnston, C. & Roth, S. (1997). *Appl. Phys. Lett.* **70**, 2891–2893.
Ma, Y., Wassdahi, N., Skytt, P., Guo, J., Nordgren, J., Johnson, P. D., Rubensson, J. E., Boske, T., Eberhardt, W. & Kevan, S. D. (1992). *Phys. Rev. Lett.* **69**, 2598–2601.
Menon, M, Andriotis, A. N. & Froudakis, G. E. (2000). *Chem. Phys. Lett.* **320**, 425–434.
Mintmire, J. W., Dunlap, B. I. & White, C. T. (1992). *Phys. Rev. Lett.* **68**, 631–634.
Morar, J. F., Himpsel, F. J., Hollinger, G., Hughes, G. & Jordan, J. L. (1985). *Phys. Rev. Lett.* **54**, 1960–1963.
Okano, K., Yamada, T., Sawabe, A., Koizumi, S., Matsuda, R., Bandis, C., Chang, W. & Pate, B. B. (1999). *Appl. Surf. Sci.* **146**, 274–279.
Perng, K., Liu, K. S. & Lin, I. N. (2000). *Diamond Relat. Mater.* **9**, 358–363.
Pickard, C. J. (1997). PhD thesis, Christ's College, Cambridge, UK.
Robertson, J., Güttler, H., Kawarada, H. & Sitar, Z. (1999). *Proceeding of the 10th European Conference on Diamond, Diamond-like Materials, Carbon Nanotubes, Nitrides, Nitrides and Silicon Carbide*. Amsterdam: Elsevier.
Saito, R., Dresselhaus, G. & Dresselhaus, M. S. (1998). *Physical Properties of Carbon Annotates*. London: Imperial College Press.
Sowers, A. T., Ward, B. L., English, S. L. & Nemanich, R. J. (1999). *J. Appl. Phys.* **86**, 3973–3982.
Won, J. H., Hatta, A., Yagyu, H., Jiang, N., Mori, Y., Ito, T., Sasaki, T. & Hiraki, A. (1996). *Appl. Phys. Lett.* **68**, 2822–2824.
Yudasaka, M. & Kikuchi, R. (1998). In *Supercarbon*, edited by S. Yoshimura & R. P. H. Chang. Berlin: Springer.
Yudasaka, M., Kikuchi, R., Ohki, Y., Ota, E. & Yoshimura, S. (1997). *Appl. Phys. Lett.* **70**, 1817–1818.